Curcumin suppresses oxidative stress via regulation of ROS/NF-κB signaling pathway to protect retinal vascular endothelial cell in diabetic retinopathy

Jiang Huang
Second Affiliated Hospital of Soochow University
Quanyong Yi
Ningbo Eye hospital
Yao Chen
second affiliated hospital of Soochow University
Yi Li
Huashan Hospital Fudan University
Guoxu Xu
Second Affiliated Hospital of Soochow University
Ji Zhang
Second Affiliated Hospital of Soochow University
Tongtong Niu
Second Affiliated Hospital of Soochow University
Yuhong You
Second Affiliated Hospital of Soochow University
Weijie Zou
Second Affiliated Hospital of Soochow University
Sicheng Qian
Second Affiliated Hospital of Soochow University
Weifeng Luo (luoweifengsz@sohu.com)
Soochow University

Research

Keywords: Curcumin, Oxidative stress, ROS/NF-κB, Diabetic retinopathy, retinal vascular endothelial cells

Posted Date: May 11th, 2020

DOI: https://doi.org/10.21203/rs.3.rs-27239/v1

Abstract

Background: Diabetic retinopathy (DR) is one of the most serious complications of diabetes mellitus and a leading blindness disease in the world. The retinal vascular endothelial cells can be damaged by oxidative stress even in the early stage of diabetic retinopathy. NF-κB is a key transcription factor in cell apoptosis and oxidative stress. Curcumin can relieve oxidative stress induced by high glucose. This study aimed to investigate the effect of curcumin on the rat retinal vascular endothelial cells (RRVECs) in DR and to deduce the possible molecular mechanism.

Methods: The cultured RRVECs were identified by both of vWF and CD31 expression.The RRVECs were divided into four groups: the normal control group, the osmolarity control group, the high glucose group and the curcumin treatment group (High glucose +Curcumin). We observed the different morphological changes in the groups by transmission electron microscopy. Oxidative stress was detected by flow cytometry. The Activation of ROS/NF-κB signal pathway was detected by electrophoretic Mobility Shift Assay (EMSA), immunohistochemistry and western-blot; the apoptosis of RRVECs was tested by flow cytometry.

Results: We found that curcumin reduced the reactive oxygen species (ROS) and relieved the apoptosis in RRVECs exposed to the high glucose by flow cytometry. We detected that the increased activity of NF-κB and phosphorylated NF-κB in RRVECs induced by high glucose concentration was significantly suppressed by curcumin. Furthermore, based on the assay quantifying the level of apoptosis-related proteins, including bcl-2 and bax, we illustrated that curcumin could decrease the apoptosis of RRVECs induced by high glucose concentration.

Conclusion: We concluded that ROS/NF-κB signaling pathway played an important role in the progress of DR and curcumin could suppress the oxidative stress via regulation of NF-κB signal to protect the RRVECs in DR.

Background

Diabetic retinopathy (DR) is one of the leading cause of blindness in working-age people in mainland China[1 2]. Pathophysiological studies have demonstrated that diabetic retinopathy brings about progressive changes of retinal microvasculature [3 4]. Typical early changes in the retinal vasculature of diabetic eyes are pericyte loss, basement membrane thickening, the retinal vascular endothelial cell (RVEC) proliferation and blood-retina barrier leakage[5 6].

Several studies [7–10] have shown that oxidative stress plays an important role in the pathogenesis of diabetic retinopathy. Oxidative stress activates multiple pathways in the cell, including signaling cascades, cell apoptosis, and transcription factors, which in turn cause the pathophysiological changes of the retinal vasculature in diabetic retinopathy. The RVECs are key participants in diabetic retinopathy. They not only supply oxygen and nutrients for the normal metabolism of the retina, but also contribute to the blood-retinal barrier that protects the retina [11 12]. NF-κB is a vital transcription factor that initiates

the transcription of genes involved in the regulation of physiological processes of the cell and its reaction to oxidative stress.An activated NF-κB can cause cell apoptosis. Some studies [13–15] have shown that NF-κB regulates the expression of angiogenic factors in vascular endothelial cells and induces neovascularization in diabetic retinopathy.

Curcumin is a yellow powder extracted from the tubers of the turmeric plant. It has well known anti-inflammatory, anti-tumor and anti-oxidation effects. Studies [16–19] found that curcumin reduced glucose intolerance and insulin resistance by its antioxidant effects and anti-inflammatory actions. Curcumin is suggested to be used as a therapeutic drug in the management of diabetes, obesity, and their associated complications [20 21]. Previous studies [22 23] have shown that curcumin has a significant antioxidant effect on retinal pigment epithelial (RPE) cells, and it inhibited RPE cell proliferation by mediating p53 signaling pathway.

However, it is unclear whether curcumin has its anti-oxidation effect on retinal vascular endothelial cells (RVECs), and its possible mechanism is still unknown. Therefore, we investigated the effects of curcumin on RRVECs exposed to high glucose concentration and analyzed the mechanism of the curcumin's action on RRVECs.

Materials And Methods

Experimental animals. Sixty cleaning grade healthy adult male Sprague-Dawley (SD) rats weighing 180±20g were obtained from the Experimental Animal Center of Soochow University. Animals were housed under standard diurnal conditions according to the guidelines established by the Animal Research: Reporting of *In Vivo* Experiments (ARRIVE). The room temperature was maintained at 20-23℃ with a relative humidity of 50-70% and the noise was kept□50dB. Before experiments, all rats were fed a basal diet for one week. For the use of experimental animals, guidelines were followed from the "Regulations on the Management of Laboratory Animals" promulgated by the National Science and Technology Commission and the Declaration of Helsinki.

Experimental materials. The following materials were obtained for this study: Curcumin [Taishi (Shanghai) Chemical Industry Development Co.,Ltd., China], trypsin (Invitrogen, USA), type II collagenase, thiazole blue (MTT), 0.04% trypan blue (Sigma, USA), rabbit monoclonal antibody to von Willebrand factor (Abcam, Cambrige, UK), rabbit anti-CD31 antibody (Abcam, Cambrige, UK), rabbit anti-NF-κB p65 antibody (Abcam, Cambrige, UK), rabbit phosphor-NF-κB p65 antibody (Cell signaling Technology, USA), rabbit anti-IKBα antibody (Abcam, Cambrige, UK), rabbit anti-Bax antibody ((Wuhan Sanying Biotechnology Co., Ltd., Hubei, China), rabbit anti-Bcl2 antibody ((Wuhan Sanying Biotechnology Co., Ltd., Hubei, China), rabbit anti-IL-1β antibody (Cell signaling Technology, USA), endothelial cell culture medium, fluorescent (Cy3) tagged goat anti-rabbit IgG (Wuhan Biosciences Co., Ltd., Hubei, China), fluorescent (FITC) tagged goat anti-rabbit IgG (Wuhan Biosciences Co., Ltd., Hubei, China), rabbit anti-phosphoglyceraldehyde Dehydrogenase (GAPDH, Hangzhou Xianzhi Biotechnology Co., Ltd., Zhejiang, China), Light shift chemiluminescent EMSA kit (Thermo Scientific, USA), bicinchoninic acid (BCA) protein

concentration determination kit, cell reactive oxygen species (ROS) detection kit (Biyuntian Biotechnology Institute, Hubei, China), diamino Diphenylamine (DAB) Chromogenic Kit (Beijing Solvay Technology Co., Ltd., China), apoptosis detection kit (Jiangsu Keyi Biotechnology Co., Ltd.,Jiangsu, China), Immunohistochemistry Kit (Beijing ZhongshanJinqiao Biotechnology Co., Ltd., China). Model IX51 inverted microscope, Eppendorf, BX53 fluorescence microscope (Olympus, Japan), Nikon E100 biomicroscope (Nikon, Japan), microplate reader (American Thermo Electron Corporation, USA), and flow cytometry (BD Biosciences, USA).

Rat retinal vascular endothelial cells (RRVECs) culture, identification and activity detection.

The RRVECs were isolated and cultured as previous described[24].The rats were anesthetized by intraperitoneally injection of 10% chloral hydrate with 3.3% ketamine.The eyes were placed in a petri dish containing iced PBS gauze, and the retinal tissues were harvested and cut into pieces. They were digested with a type II collagenase for 30 minutes at 37°C, and the digestive fluid was absorbed. The retinal tissues were then transferred to solution A consisting of NaCl, KCl, CaCl, $MgCl_2$ and mannitol, and the osmotic pressure was adjusted to 310mosmol. The retinal microvessels were cut into quadrants and placed in a glass-bottomed chamber. A coverslip was then placed over the retina, so that the microvessels adhered to the coverslip. The cells were sieved through two stainless steel mesh of 100 μm pore size, and the eluate was gathered.The eluate was centrifuged at 1500 r/m for 5 minutes at room temperature and the supernatant was removed.The precipitate after centrifugation was added to Dulbecco's modified Eagle's medium (DMEM) containing $100x10^3$ U/L heparin sodium and fetal bovine serum. It was inoculated on a 24-well culture plate, and then placed in a 37°C, 5% CO_2 incubator and periodically exchanged. Retinal vascular endothelial cells were observed under an inverted microscope before the medium was changed. The labeled hybrid cells were removed with a scraper. Following this, the cell viability was assessed using trypan blue staining.

The 4th generation rat RRVECs were inoculated on gelatin-coated coverslips at a density of $1x10^4$ cells/ml and cultured for 24 h. After the cells were adherent, the coverslips were removed and immunofluorescence staining was used to identify the cells with vWF and anti-CD31 antibody at 4℃ over night. In the negative control group, PBS was used instead of the primary antibodies. Cy3 and FITC as the secondary antibodies were added to the working solution at 37°C for incubation, respectively. The color was observed under a fluorescence microscope, and images were collected. Cy3 emits green fluorescence and FITC emits red fluorescence as a positive expression.

Grouping of Cells.

The RRVECs were divided into normal control group, osmolarity control group, high glucose group and curcumin treatment group (High glucose +Curcumin).The glucose concentration in the normal control group was 5.5mmol/L. The osmotic control group had 5.5mmol/L glucose and 19.5mmol/L mannitol to a final concentration of 25mmol/L. In the high glucose group, the glucose was added at a concentration

of 25mmol/L for 72h. In the treatment group was exposed to glucose at a concentration of 25 mmol/L for first 72 h and then treated with 30 μmol/L curcumin for 48h.

Morphological changes in RRVECs by transmission electron microscopy.

The cellular morphological changes in each group were detected by the transmission electron microscopy (TEM). The cells were collected via centrifugation (800rpm, 5minutes), and washed with PBS and fixed with 1% paraformaldehyde and then with 2% glutaraldehyde for 12hours. Afterwards, the fixed cells were treated with 1% osmium tetroxide for 3hours, dehydrated through an ethanol gradient, and embedded in Araldite. Ultrathin sections were stained with uranyl acetate and lead citrate, and examined by the TEM (Tecnai, FEI). The EDX ChemSTEM analysis system was used to take TEM images at magnifications of 2500x.

Detection of intracellular superoxide by ROS Assay.

Flow cytometry was used to detect reactive oxygen species (ROS) levels in RRVEC.A single suspension of cells was prepared from each group of cells, inoculated evenly in a 6-well plate at the cell density of 2×10^5 cells/well, and cultured overnight at 37° C in 5% CO_2 saturation humidity. The cells were then digested with 0.25% trypsin without ethylenediaminetetraacetic acid. The digestion was stopped and the digested cells were centrifuged.The supernatant was discarded and the cells were rinsed twice with PBS. Following the instructions for the operation of the DCFH-DA cell ROS kit, the flow cytometry was performed.

Flow cytometry analysis.

Flow cytometry was used to analyze the apoptosis of RRVECs in each group. Each group of cells was cultured at 37° C in a 5% CO_2 incubator for 72 hours.A single suspension of cells was prepared from each sample, and incubated in the dark for 15 minutes at room temperature. Solutions of Annexin (5 μl) and propidium iodide (1μl) were added to cell suspension and incubated in the dark at room temperature for 15 minutes. After the incubation, 400 μl of annexin binding buffer was added, and finally analyzed by flow cytometry.

Immunohistochemistry

The expression of NF-κB p65 in RRVECs was detected using immunohistochemical staining described previously[[25]]. The cells were seeded on a 6-well plate cover glass. After 24 hours, the serum-free medium was replaced and the culture was continued for 24 hours. The slides were removed,washed with PBS and rabbit anti-human NF-κB p65 polyclonal antibody was added. The procedure was performed according to the fungal avidin-peroxidase ligation immunohistochemistry kit. The cytoplasm showing yellow or brown-yellow staining was considered positive. Ten high-power field of each slice was observed and photographed under a microscope.The images were analyzed using a digital image analysis system. The relative expression level of the target protein was calculated by the average value of the positive cells.

Detection of NF-κB Activity by EMSA.

The Electrophoretic Mobility Shift Assay (EMSA) was performed using an NF-κB EMSA Kit (Thermo Scientific, USA). The nucleoproteins in the RRVEC were extracted using a Nucleoprotein and Cytoplasmic Protein Extraction Kit according to the manufacturer's protocol. The following DNA sequences were synthesized for EMSA analysis:

consensus oligonucleotides of NF-κB p65: 5'-AGTTGAGGGGACTTTCCCAGG C-3' 3'-TCAACTCCCCTGAAAGGGTCCG-5'. The NF-κB/DNA binding activity was determined with Light Shift Chemiluminescent EMSA kit. The detailed procedure of EMSA has been described previously[[26 27]].

Western-Blotting.

The expression of NF-κBp65, phosphorylated NFκBp65, IKB-α, IL-1β, Bax and Bcl-2 in each group of RRVEC were detected by western blot. The total protein was extracted from the cells and the target proteins were detected. Protein samples and standard proteins diluted in PBS were respectively added to 96-well plates. Two parallel wells were set for each standard sample. Three parallel wells were set for the sample to be tested, and 20 μl samples was added to each well. Two parallel wells with PBS were blank controls. The liquid mixture of BCA protein with a ratio of 50:1 was added to each well in a 96-well plate, and incubated at 37° C for 30 minutes in the dark.

The microwell plate was read at a wavelength of 568nm with a microplate reader. The linear regression equation was calculated based on the standard protein concentration and the corresponding the value. According to the value of the protein sample, the regression equation was used to calculate the sample protein concentration. The extracted protein sample and five-time protein loading buffer were placed in boiling water for 10 minutes to perform protein denaturation. Electrophoresis and transfer were performed according to the literature method[[28]]. The membrane was blocked and the primary antibody was added to incubate overnight at 4°C (GAPDH: 1:1000; NF-κBp65:1:10000; pNF-κBp65:1:1000; IKB-α:1:1000; IL-1β:1:1000; Bcl-2: 1:1000; Bax: 1:2000). After washing the membrane 5-6 times, the corresponding secondary antibody was added. After the membrane was washed, the films with chemiluminescence were developed, fixed, and rinsed. BandScan was used to analyze the film gray value. It was repeated 3 times.

Statistical methods

Statistical software SPSS20.0 was used for statistical analysis. The data were distributed by the Shapiro-Wilk test, and the cell apoptosis rate was expressed as a percentage. Other experimental data were expressed as the mean ± standard deviation (`x±s); the average between groups was homogeneity using the variance by Levene test, and analysis of variance multiple comparisons(ANOVA) with Bonferroni's multiple comparison test was performed to analyze the data in more than two groups of variables. $P<0.05$ was considered statistically significant.

Results

The isolated RRVECs were patina-like monolayer adherent growth after one week, when observed under an inverted microscope. The cultured cells were strongly positive for vWF and CD31 expression which are endothelial cell specific markers (Figure 1).

A Inverted phase contrast microscope image, RRVECs cultured for 7 days showed a paving stone-like growth; B Immunofluorescence microscope image, the green fluorescence of the cytoplasm by vWF immunofluorescence; C Immunofluorescence microscope image, the red fluorescence of the cytoplasm by CD31. All the nuclei were stained with DAPI.

Figure 1 Inverted phase microscopy and immunofluorescence microscopy images of RRVECs.

(A) Inverted phase contrast microscope image, RRVECs cultured for 7 days showed a paving stone-like growth; (B) Immunofluorescence microscope image, the green fluorescence of the cytoplasm by vWF immunofluorescence; (C) Immunofluorescence microscope image, the red fluorescence of the cytoplasm by CD31. All the nuclei were stained with DAPI.

The ultrastructure changes in RRVECs were examined by transmission electron microscopy to detect whether curcumin could reduce the damage caused by high glucose concentration. As were shown in Figure2A-D, a significant increase of retinal capillary basement membrane thickness, swollen cell and shrunken nucleus in the high glucose group compared with the normal control group were observed.However,with the treatment of curcumin, an obvious reduction in retinal capillary basement membrane thickness and other abnormal structure including swollen cell and shrinkage of cellular nucleus were detected in RRVECs.

Figure2. The ultrastructure changes of RRVECs detected by transmission electron microscopy

A. Normal RRVECs of the control group. (B) RRVECs of the osmotic

control group. (C) High glucose group. A significant increase of the structural abnormalities including swollen cell and shrunken nucleus in RRVECs can be observed at the dose of 25mmol/L glucose. The bold black arrow shows the swollen cellular and the thin black arrow shows the shrinkage cellular nucleus. (D)Exposed to curcumin at the concentration of 30μmol/L, a significant reduction in the structural abnormalities induced by high glucose can be observed in the RRVECs, compared with those in high glucose group without curcumin treatment. The bold black arrow shows the swollen cell and the thin black arrow shows thrunken cellular nucleus.

Figure3A and 3B showed that the relative levels of ROS of RRVECs in control group, osmotic control group, high glucose group and curcumin treatment group were significantly different ($p \leq 0.001$).

Compared with the control group, the relative content of ROS in RRVECs was significantly increased in the high glucose group ($p \leq 0.001$). Compared with the high glucose group, the relative content of ROS in the RRVEC of the curcumin treatment group was significantly decreased, and the difference was statistically significant ($p \leq 0.001$) (Figure3A, B).

Annexin V-FITC/PI double staining results revealed that the apoptosis rate of RRVECs in the control group, high glucose group and curcumin treatment group was statistically significant ($p \leq 0.001$). Compared with the control group, the high glucose group showed significantly increased RRVECs apoptosis rate($p \leq 0.001$). Furthermore, after the curcumin treatment with 30umol/L in RRVECs, the cell apoptosis was decreased dramatically($p<0.05$) (Figure3C, D).

Figure3 Comparison of relative ROS content and apoptosis rate of RRVECs by flow cytometry in each group.

A. The relative ROS content flow chart; (B) ROS content of RRVECs histogram; *$p<0.05$; ** $p<0.01$
B. Cell apoptosis flow chart; (D) Cell apoptosis histogram *$p<0.05$; ** $p<0.01$

The NF-κB signaling was detected by immunohistochemistry, western-blot and electrophoretic mobility shift assay (EMSA). As illustrated in the Figure4(A-D), the expression of NF-κB p65 protein was positive in the cytoplasm of RRVECs in the control group (Fig4A). The positive expression of NF-κB p65 protein was found in the nucleus and cytoplasm of RRVECs in both high glucose group and curcumin treatment group (Fig.4C, D). As compared with the control group, the expression of NF-κB was significantly increased in high glucose group ($p<0.01$). However, the expression of NF-κB was declined sharply in the curcumin treatment group compared to the high glucose group ($p<0.05$). (Fig4E). The results of the EMSA and western-blot tests demonstrated a similar results as immunohistochemistry. The binding activity of transcription factor NF-κB was modulated by the treatment of curcumin, as is shown in Figure5A. In the high glucose group, the activity of NF-κB binding DNA was increased. However, when the RRVECs were incubated with the curcumin, the NF-κB activity was decreased.

Figure4. The detection of NF-κB signal activity and protein expression of RRVECs in each group by immunohistochemistry.

(A) NF-κB protein expression detected by immunohistochemical staining in normal RRVECs; (B) NF-κB protein expression detected by immunohistochemical staining in osmotic control group; (C) NF-κB protein expression detected by immunohistochemical staining in RRVECs exposed to high glucose concentration; (D) NF-κB protein expression detected by immunohistochemical staining in the curcumin treatment group; (E) Histogram of relative NF-κB expression in each group. *$p<0.05$ **$p<0.01$

Furthermore, the activity of NF-κBp65 was detected in RRVECs by Western-Blot test.As shown in Figure5B and 5C, when RRVECs were exposed to 25μmol/L of glucose, both the expression of NF-κB and phosphorylated NF-κB were increased significantly, compared with the normal control group.With the treatment of curcumin, the expression of NF-κB and pNF-κB were declined significantly compared with the high glucose group, respectively ($p<0.05$, $p<0.01$) (Fig5C).

Figure5. The detection of NF-κB signal activity and protein expression of RRVECs in each group by EMSA and western-blot tests.

(A) NF-κB/DNA binding activity was examined by EMSA;

(B) NF-κBp65 protein and phosphorylated NF-κBp65 protein expression detected by Western-Blot assay in each group; (C) Histogram of relative NF-κBp65 and phosphorylated NF-κBp65 expression in each group. *$p<0.05$ **$p<0.01$

The results of the western-blot analysis showed that in high glucose group, the levels of IKb-α, IL-β and Bax were dramatically increased, whereas, the expression of Bcl-2 was reduced in RRVECs, compared with the control group. When it was treated with curcumin, the expression level of IKb-α, IL-β and Bax were decreased, whereas Bcl-2 expression increased(Fig6A, B).

Figure6. Comparison of IKb-α、IL-β、Bax and Bcl-2 proteins expression in RRVECs in each group. *P<0.05 **P<0.01

A. Electropherogram of IKb-α、 IL-β、Bax and Bcl-2 protein expressions; (B) Histogram of IKb-α、IL-β、Bax and Bcl-2 protein expressions

Discussion

Gupta et al[29] demonstrated that oral administration of curcumin to diabetic rats increased the expression of antioxidant enzymes and superoxide dismutase in rat retina after 16 weeks, and inhibited the expression of TNF-α and VEGF. The reduction of capillary basement membrane thickening, but the study did not involve the possible cellular pathophysiological mechanisms. This study showed that RRVECs exposed to glucose at 25 mmol/L concentration for 72 h were activated and a large number of intracellular ROS was produced. Then, when they were treated with 30 μmol/L curcumin for 48 h, the production of intracellular ROS was significantly reduced. This suggests that curcumin can obviously resist the oxidative stress caused by high glucose. The results of flow cytometry test showed that curcumin had a significant inhibitory effect on the apoptosis of RRVECs induced by oxidative stress.

Using transmission electron microscopy, the morphological characteristics of cellular abnormality were detected in RRVECs induced by high glucose. It showed that a significant increase in retinal capillary basement membrane thickness compared to normal control RRVECs and osmolarity control group. The nucleus and cytoplasm of RRVECs at high glucose displayed cellular swelling and cellular nucleus shrinking. After curcumin treatment, it was demonstrated that curcumin ameliorated the abnormal change of cellular structure in RRVECs.

The combined analysis of immunohistochemistry, EMSA and western-blot tests of NF-κB showed that the level of phosphorylated NF-κB and NF-κB were significantly elevated, when RRVECs exposed to the high glucose. However, after treatment with curcumin, the level of phosphorylated NF-κB and NF-κB were distinctly decreased. Immunohistochemical staining showed that when the RRVECs were induced by high glucose, the expression of NF-κB p65 in the nucleus of the cells was significantly increased, while the expression of NF-κB p65 in the cytoplasm was decreased. It was demonstrated that NF-κB in the cytoplasm of RRVECs entered into the nucleus and exerted transcriptional activity. With the treatment of curcumin, the expression of NF-κB p65 was decreased in the cytoplasm of RRVECs,meanwhile, the NF-κB in cytoplasm were inhibited from emtering to the nucleus. The western-blot assay had the consistent results for the expressions of NF-κB and pNF-κB. The results indicated that curcumin could block the signal of NF-κB which may reduce the oxidative stress response of high glucose-induced RRVECs. The results of EMSA

Presented the same results as well. In the high glucose group, the activity of NF-κB/DNA binding was increased, whereas, after curcumin treatment, the NF-κB activity was significantly declined. These results demonstrated that oxidative stress induced by high glucose could activate NF-κB as well as the phosphorylated NF-κB, and curcumin could suppress the activity of NF-κB by anti-oxidative stress to protect the RRVECs exposed to high glucose.

Bcl-2 and Bax regulated by NF-κB are the suppressor of apoptosis and pro-apoptosis gene, respectively. The promoter region of Bcl-2 gene contains a binding site of NF-κB, and NF-κB can directly up-regulate or promote the expression of Bcl-2 through other pathways [30–32]. To study the specific molecular mechanism of curcumin in anti-oxidative stress, we observed the expression of Bcl-2 and Bax in RRVECs exposed to high glucose.

We detected that the protein expression of Bax was dramatically increased, but the Bcl-2 protein expression was diminished after the RRVECs were induced by high glucose.With the treatment of curcumin, the expressions of NF-κB and Bax were declined obviously and the expression of Bcl-2 was raised apparently. The consistency of the expressions of NF-κB p65, Bcl-2 and Bax protein in our study showed that RRVECs induced by high glucose could activate NF-κB pathway, which resulted in the decline of the expression of Bcl-2 protein and incline of the expression of Bax protein. However, curcumin could suppress this process.

IL-1β,which is regulated by the transcription factor NF-κB is a major pro-inflammatory cytokine involved in the pathogenesis of oxidative stress. The binding sites of NF-κB have been identified in the promoter of

IL-1β. Activating the NF-κB pathway can induce the IL-1β expression lead to the recruitment of inflammatory cells, and increase of the activity of inflammatory mediators[33–35]. The inactive form of IL-1β(IL-1β 31KDa) must be cleaved into the active form (IL-1β 17KDa) and then release from the cell. Moreover, in this study, it was demonstrated that the IL-1β 17KDa was increased significantly in RRVECs incubated with high glucose. However, when it was treated with curcumin, the expression of IL-1β 17KDa was declined.

Conclusion

The results of this study indicate that curcumin can inhibit the production of ROS and the occurrence of apoptosis in RRVEC induced by high glucose. The possible mechanism might be the suppression of NF-κB expression leads to the increased expression of Bcl-2, and consequently, the cellular apoptosis is alleviated. Therefore, it can be suggested that curcumin can protect the retinal vascular endothelial cells by inhibiting NF-κB pathway and antagonizing oxidative stress. The more precise and profound mechanism remains to be further confirmed by extensive molecular biology studies.

Abbreviations List

DR, Diabetic retinopathy; RRVECs, rat retinal vascular endothelial cell; RPE , retinal pigment epithelial; MTT, thiazole blue; DMEM, Dulbecco's modified Eagle's medium; TEM, transmission electron microscopy; ROS, reactive oxygen species; BCA, bicinchoninic acid; DAB, diamino Diphenylamine; EMSA, Electrophoretic Mobility Shift Assay

Declarations

Data Availability

The data used to support the findings of this study are included within the article.

Competing interests

The authors have no conflicts of interest related to this research.

Acknowledgments

Not applicable.

Funding

This work was supported by the Second affiliated hospital of Soochow University Research fund project (SDFEYBS1903); National Natural Science Foundation of China (No. 81671270); the Second affiliated hospital of Soochow University preponderant clinic discipline group project funding (XKQ2015002).

Authors' contributions

In this work, JH, YL and QY conceived the study and designed the experiments. JH, YL, QY and SQ performed the experiments. YC and GX contributed to the data collection; JZ, TN, WZ and YY performed the data analysis and interpreted the results. JH and WL wrote the manuscript; WL contributed to the critical revision of article. All authors read and approved the final manuscript.

Ethics approval and consent to participate

This study was conducted in accordance with the "Guide for the Care and

Use of Laboratory Animals" prepared by the National Academy of Sciences and published by the National Institutes of Health and with the approval by the Ethical Committee on Animal Research at second affiliated hospital of Soochow University (Suzhou, Jiangsu, China).

Consent for publication

Not applicable.

Availability of data and materials

The datasets used and analysed during the current study are included in this published article.

References

1. Wang FH, Liang YB, Zhang F, et al. Prevalence of Diabetic Retinopathy in Rural China: The Handan Eye Study. Ophthalmology. 2009;116(3):461–67. doi:10.1016/j.ophtha.2008.10.003[published Online First: Epub Date]|.
2. Xie XW, Xu L, Wang YX, Jonas JB. Prevalence and associated factors of diabetic retinopathy. The Beijing Eye Study 2006. Graefes Arch Clin Exp Ophthalmol. 2008;246(11):1519–26. doi:10.1007/s00417-008-0884-6[published Online First: Epub Date]|.
3. Alder VA, Su EN, Yu DY, Cringle SJ, Yu PK. Diabetic retinopathy: early functional changes. Clin Exp Pharmacol Physiol. 1997;24(9–10):785–8.
4. De Abreu JRF, Silva R, Cunhavaz J. The Blood-Retinal Barrier in Diabetes During Puberty. Arch Ophthalmol. 1994;112(10):1334–38.
5. Cunhavaz J, Leite E, Sousa J, De Abreu JRF. Blood-retinal barrier permeability and its relation to progression of retinopathy in patients with type 2 diabetes. A four-year follow-up study. Graefes Arch Clin Exp Ophthalmol. 1993;231(3):141–45.
6. Sone H, Deo BK, Kumagai AK. Enhancement of glucose transport by vascular endothelial growth factor in retinal endothelial cells. Invest Ophthalmol Vis Sci. 2000;41(7):1876–84.
7. Roy S, Kern TS, Song B, Stuebe C. Mechanistic Insights into Pathological Changes in the Diabetic Retina: Implications for Targeting Diabetic Retinopathy. Am J Pathol. 2017;187(1):9–19 doi.

2[published Online First: Epub Date]|.. (:: 10.1016/j.ajpath.2016.08.02.

8. Stitt AW, Curtis TM, Chen M, et al. The progress in understanding and treatment of diabetic retinopathy. Progress in Retinal Eye Research. 2016;51:156–86. doi:https://doi.org/10.1016/j.preteyeres.2015.08.001[published Online First: Epub Date]|.
9. Tonade D, Liu H, Palczewski K, Kern TS. Photoreceptor cells produce inflammatory products that contribute to retinal vascular permeability in a mouse model of diabetes. Diabetologia. 2017;60(10):2111–20. doi:10.1007/s00125-017-4381-5[published Online First: Epub Date]|.
10. Fan Y, Qiao Y, Huang J, Tang M. Protective Effects of Panax notoginseng Saponins against High Glucose-Induced Oxidative Injury in Rat Retinal Capillary Endothelial Cells. Evidence-based Complementary Alternative Medicine. 2016;2016:5326382–82.
11. Ahsan H. Diabetic retinopathy–biomolecules and multiple pathophysiology. Diabetes Metabolic Syndrome: Clinical Research Reviews. 2015;9(1):51–4.
12. Kady N, Yan Y, Salazar T, et al. Increase in acid sphingomyelinase level in human retinal endothelial cells and CD34 + circulating angiogenic cells isolated from diabetic individuals is associated with dysfunctional retinal vasculature and vascular repair process in diabetes. Journal of Clinical Lipidology. 2017;11(3):694–703.
13. Ahmed S, Mundhe N, Borgohain MP, et al. Diosmin Modulates the NF-kB Signal Transduction Pathways and Downregulation of Various Oxidative Stress Markers in Alloxan-Induced Diabetic Nephropathy. Inflammation. 2016;39(5):1783–97.
14. Kowluru RA, Mishra M, Kumar B. Diabetic retinopathy and transcriptional regulation of a small molecular weight G-Protein, Rac1. Exp Eye Res. 2016;147:72–7.
15. Rojas M, Lemtalsi T, Toque HA, et al. NOX2-Induced Activation of Arginase and Diabetes-Induced Retinal Endothelial Cell Senescence. Antioxidants. 2017;6(2):43.
16. Aggarwal BB, Deb L, Prasad S. Curcumin differs from tetrahydrocurcumin for molecular targets, signaling pathways and cellular responses. Molecules. 2014;20(1):185–205.
17. Ghosh S, Banerjee S, Sil PC. The beneficial role of curcumin on inflammation, diabetes and neurodegenerative disease: A recent update. Food Chem Toxicol. 2015;83:111–24.
18. Heger M, Van Golen RF, Broekgaarden M, Michel MC. The Molecular Basis for the Pharmacokinetics and Pharmacodynamics of Curcumin and Its Metabolites in Relation to Cancer. Pharmacol Rev. 2013;66(1):222–307.
19. Prasad S, Gupta SC, Tyagi AK, Aggarwal BB. Curcumin, a component of golden spice: from bedside to bench and back. Biotechnol Adv. 2014;32(6):1053–64.
20. Chuengsamarn S, Rattanamongkolgul S, Luechapudiporn R, Phisalaphong C, Jirawatnotai S. Curcumin Extract for Prevention of Type 2 Diabetes. Diabetes Care. 2012;35(11):2121–27.
21. Hassan HA, Elgharib NE. Obesity and Clinical Riskiness Relationship: Therapeutic Management by Dietary Antioxidant Supplementation–a Review. Appl Biochem Biotechnol. 2015;176(3):647–69.

22. Vasquez DH, Diaz MF, Sanhueza C, et al. Curcumin inhibits both hypoxia-induced VEGF up regulation in retinal pigment epithelium cells and angiogenesis of choroidal vascular cells. Invest Ophthalmol Vis Sci. 2014;55(13):603–03.
23. Zhu W, Wu Y, Meng Y, et al. Effect of curcumin on aging retinal pigment epithelial cells. Drug Design Development Therapy. 2015;9:5337–44.
24. Greenwood J. Characterization of a rat retinal endothelial cell culture and the expression of P-glycoprotein in brain and retinal endothelium in vitro. J Neuroimmunol. 1992;39(1):123–32.
25. Bhat OM, Kumar PU, Giridharan NV, Kaul D, Kumar MJM, Dhawan V. Interleukin-18-induced atherosclerosis involves CD36 and NF-κB crosstalk in Apo E−/− mice. J Cardiol. 2015;66(1):28–35.
26. Juvekar A, Ramaswami S, Manna S, Chang T, Zubair A, Vancurova I. Electrophoretic mobility shift assay analysis of NFκB transcriptional regulation by nuclear IκBα. Methods of Molecular Biology. 2012;809:49–62.
27. Kitaoka Y, Isenoumi K, Kumai T, Kobayashi S, Ueno S. Nitric Oxide Inhibits NMDA-Induced Activation of NF-kB in Rat Retina. Invest Ophthalmol Vis Sci. 2003;44(13):4577–77.
28. Wei C, Li L, Gupta S. NF-κB-mediated miR-30b regulation in cardiomyocytes cell death by targeting Bcl-2. Mol Cell Biochem. 2014;387:135–41.
29. Gupta SK, Kumar B, Nag TC, et al. Curcumin prevents experimental diabetic retinopathy in rats through its hypoglycemic, antioxidant, and anti-inflammatory mechanisms. J Ocul Pharmacol Ther. 2011;27(2):123–30.
30. Mohammadi A, Yaghoobi MM, Gholamhoseyniannajar A, Kalantarikhandani B, Sharifi H, Saravani M. HSP90 inhibitor enhances anti-proliferative and apoptotic effects of celecoxib on HT-29 colorectal cancer cells via increasing BAX/BCL-2 ratio. Cell Mol Biol (Noisy-le-grand). 2016;62(12):62–7.
31. Wang Q, Liu S, Tang Y, Liu Q, Yao Y. MPT64 protein from Mycobacterium tuberculosis inhibits apoptosis of macrophages through NF-kB-miRNA21-Bcl-2 pathway. PLOS ONE 2014;9(7).
32. Wang Y, Wang R, Wang Y, Peng R, Wu Y, Yuan Y. Ginkgo biloba extract mitigates liver fibrosis and apoptosis by regulating p38 MAPK, NF-κB/IκBα, and Bcl-2/Bax signaling. Drug Design Development Therapy. 2015;9:6303–17.
33. Hiscott J, Marois J, Garoufalis J, et al. Characterization of a functional NF-kappa B site in the human interleukin 1 beta promoter: evidence for a positive autoregulatory loop. Mol Cell Biol. 1993;13(10):6231–40. doi:10.1128/mcb.13.10.6231[published Online First: Epub Date]|.
34. Caradonna F, Cruciata I, Schifano I, et al. Methylation of cytokines gene promoters in IL-1β-treated human intestinal epithelial cells. Inflamm Res. 2018;67(4):1–11.
35. Scholz CC, Cavadas MAS, Tambuwala MM, et al. Regulation of IL-1β–induced NF-κB by hydroxylases links key hypoxic and inflammatory signaling pathways. Proc Natl Acad Sci USA. 2013;110(46):18490–95.

Figures

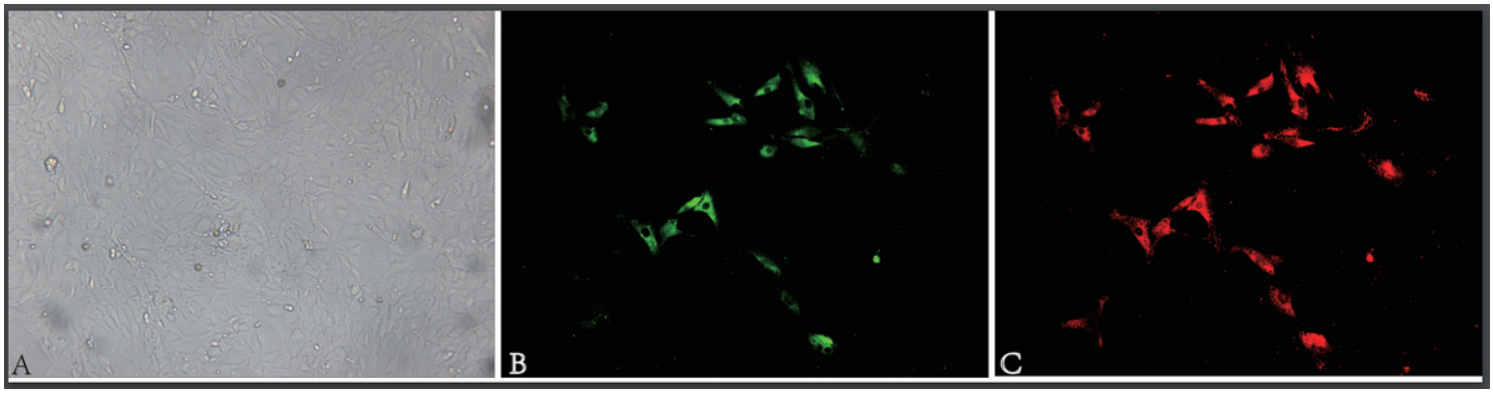

Figure 1

Inverted phase microscopy and immunofluorescence microscopy images of RRVECs. (A) Inverted phase contrast microscope image, RRVECs cultured for 7 days showed a paving stone-like growth; (B) Immunofluorescence microscope image, the green fluorescence of the cytoplasm by vWF immunofluorescence; (C) Immunofluorescence microscope image, the red fluorescence of the cytoplasm by CD31. All the nuclei were stained with DAPI.

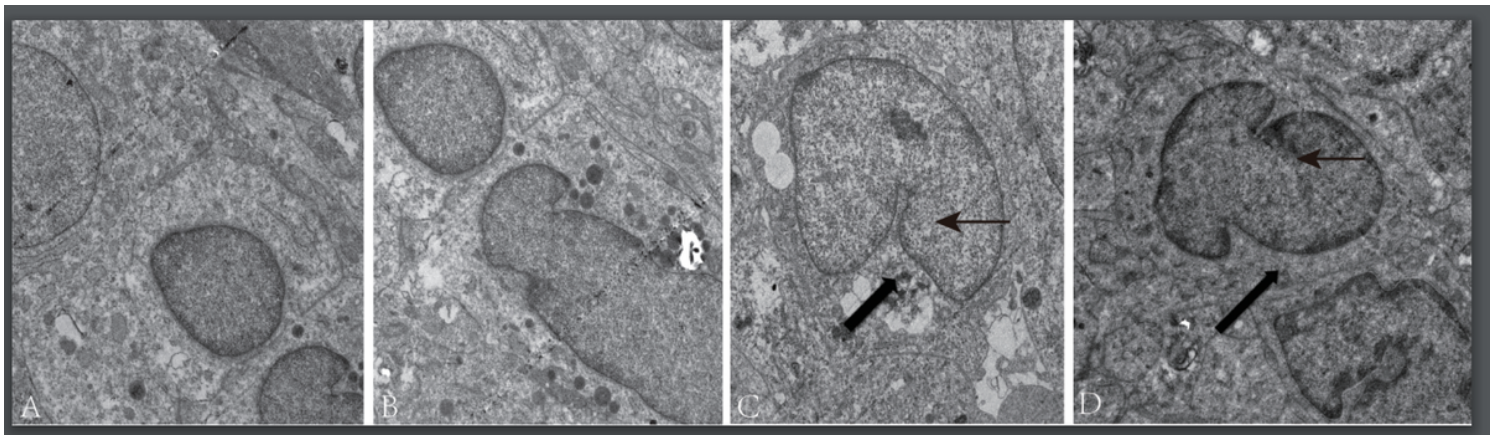

Figure 2

The ultrastructure changes of RRVECs detected by transmission electron microscopy A. Normal RRVECs of the control group. (B) RRVECs of the osmotic control group. (C) High glucose group. A significant increase of the structural abnormalities including swollen cell and shrunken nucleus in RRVECs can be observed at the dose of 25mmol/L glucose. The bold black arrow shows the swollen cellular and the thin black arrow shows the shrinkage cellular nucleus. (D)Exposed to curcumin at the concentration of 30μmol/L, a significant reduction in the structural abnormalities induced by high glucose can be observed in the RRVECs, compared with those in high glucose group without curcumin treatment. The bold black arrow shows the swollen cell and the thin black arrow shows thrunken cellular nucleus.

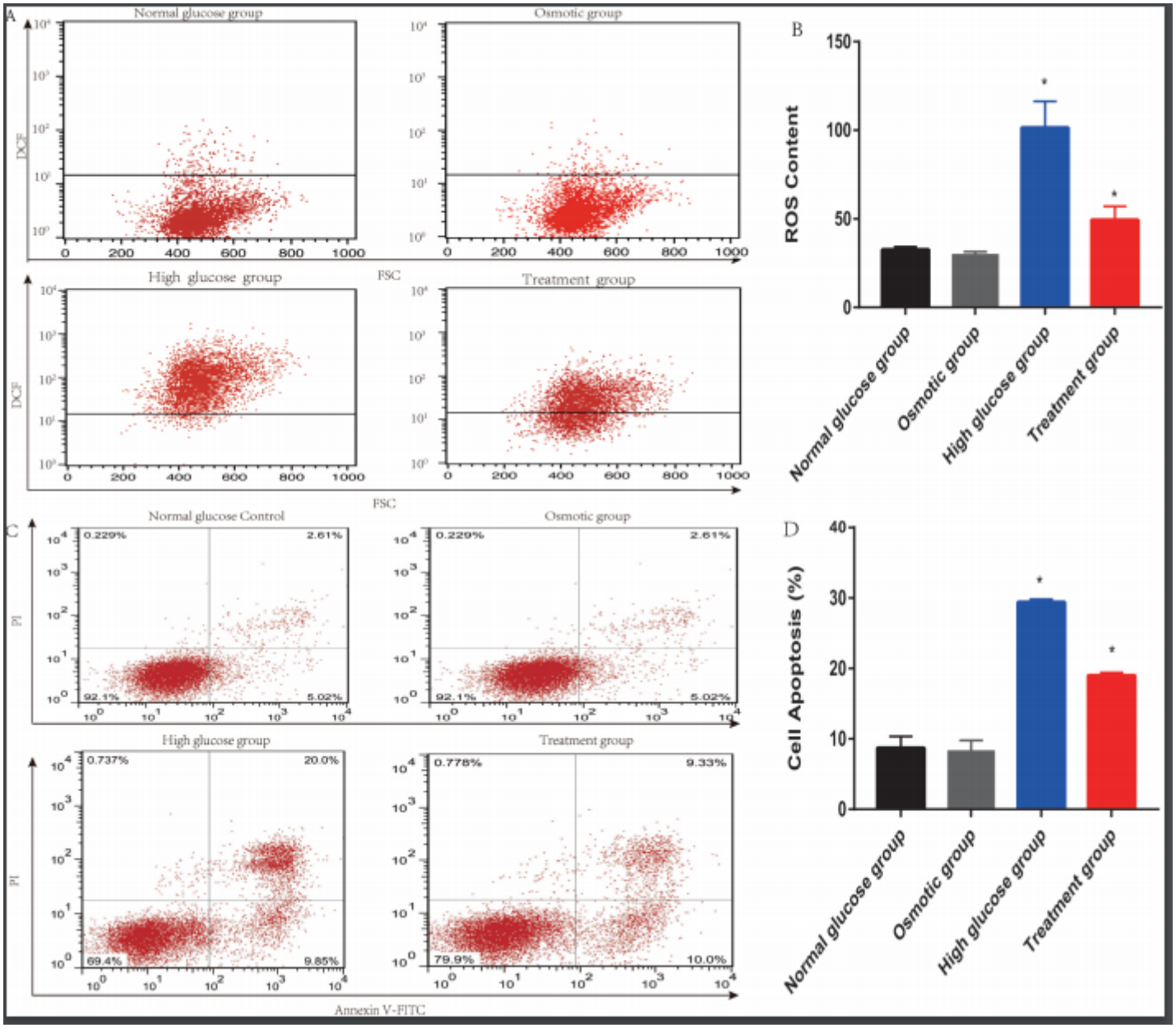

Figure 3

Comparison of relative ROS content and apoptosis rate of RRVECs by flow cytometry in each group. (A) The relative ROS content flow chart; (B) ROS content of RRVECs histogram; *p<0.05; ** p<0.01 (B) Cell apoptosis flow chart; (D) Cell apoptosis histogram *p<0.05; ** p<0.01

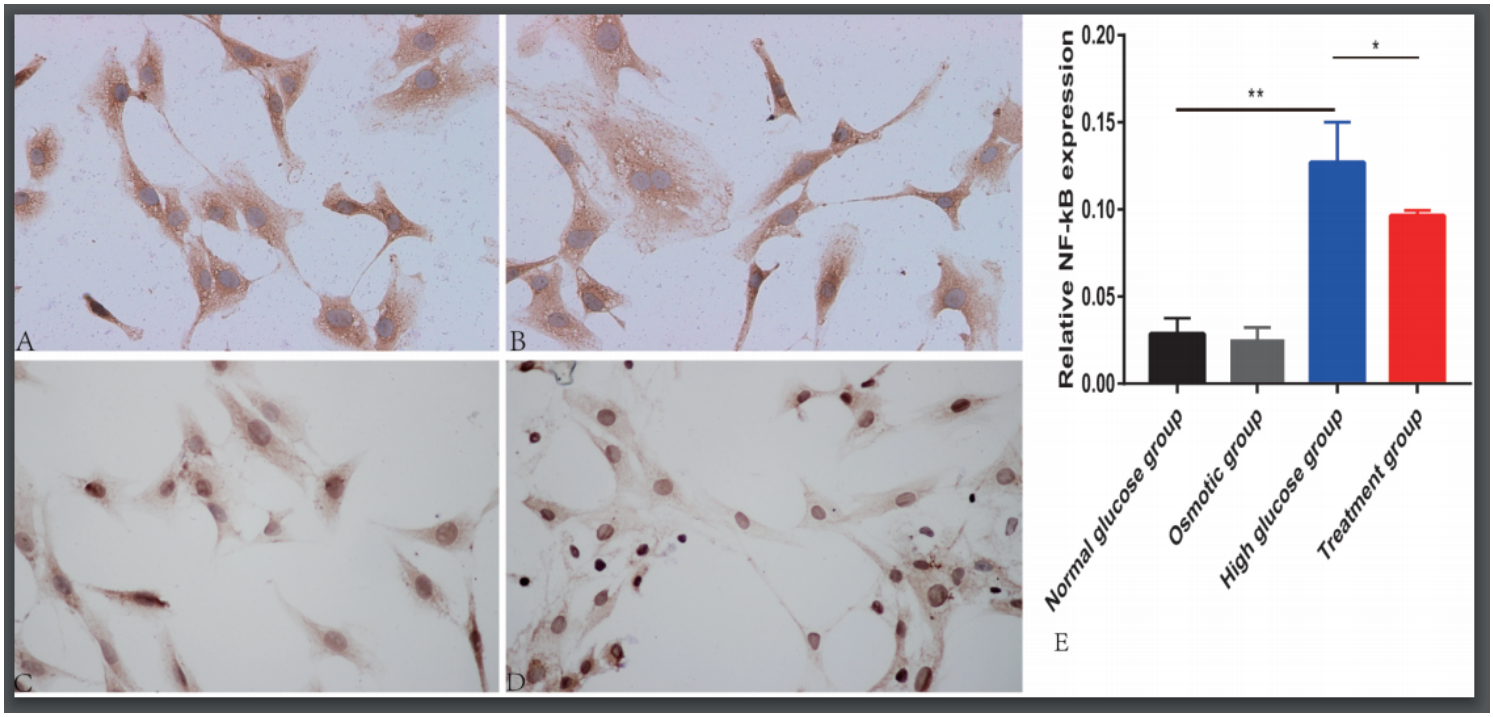

Figure 4

The detection of NF-κB signal activity and protein expression of RRVECs in each group by immunohistochemistry. (A) NF-κB protein expression detected by immunohistochemical staining in normal RRVECs; (B) NF-κB protein expression detected by immunohistochemical staining in osmotic control group; (C) NF-κB protein expression detected by immunohistochemical staining in RRVECs exposed to high glucose concentration;(D) NF-κB protein expression detected by immunohistochemical staining in the curcumin treatment group; (E) Histogram of relative NF-κB expression in each group. *p<0.05 **p<0.01

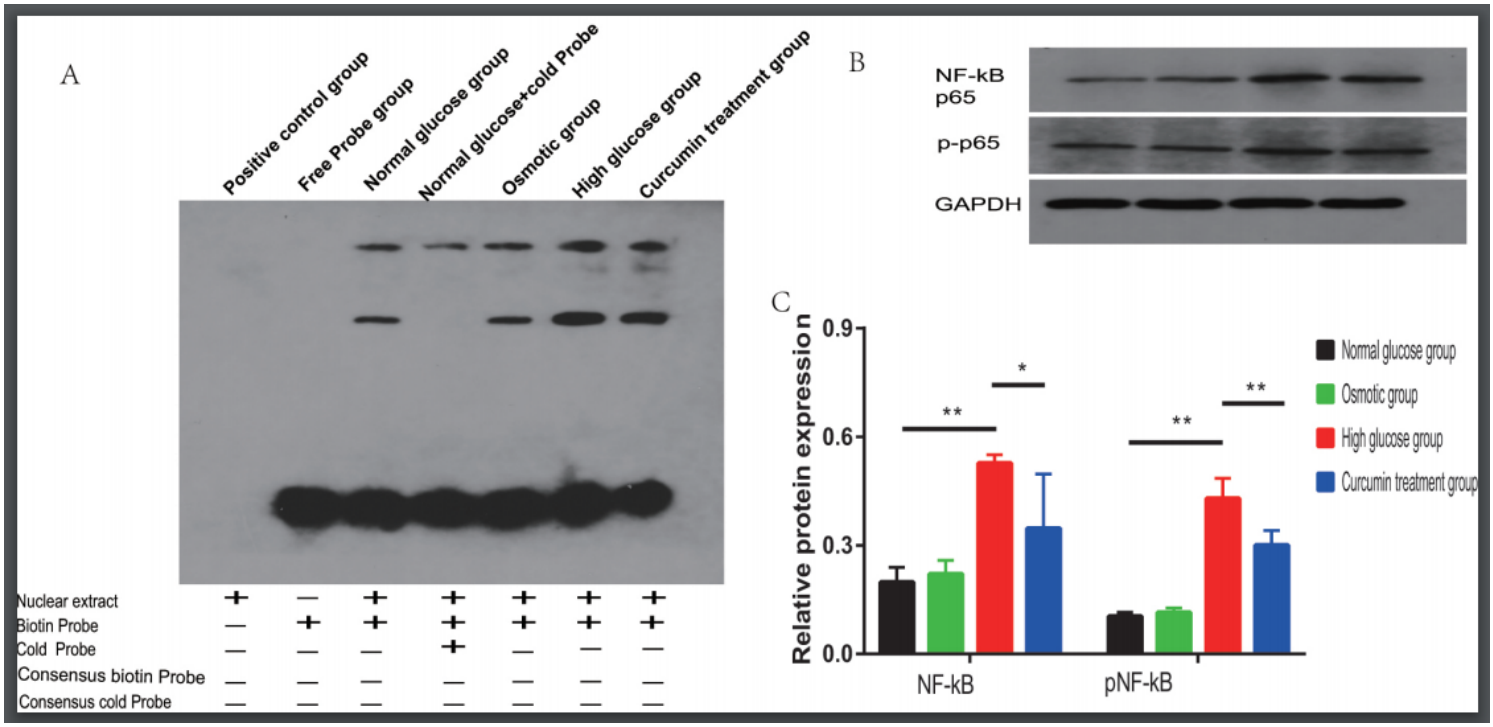

Figure 5

The detection of NF-κB signal activity and protein expression of RRVECs in each group by EMSA and western-blot tests. (A) NF-κB/DNA binding activity was examined by EMSA; (B) NF-κBp65 protein and phosphorylated NF-κBp65 protein expression detected by Western-Blot assay in each group; (C) Histogram of relative NF-κBp65 and phosphorylated NF-κBp65 expression in each group. *p<0.05 **p<0.01

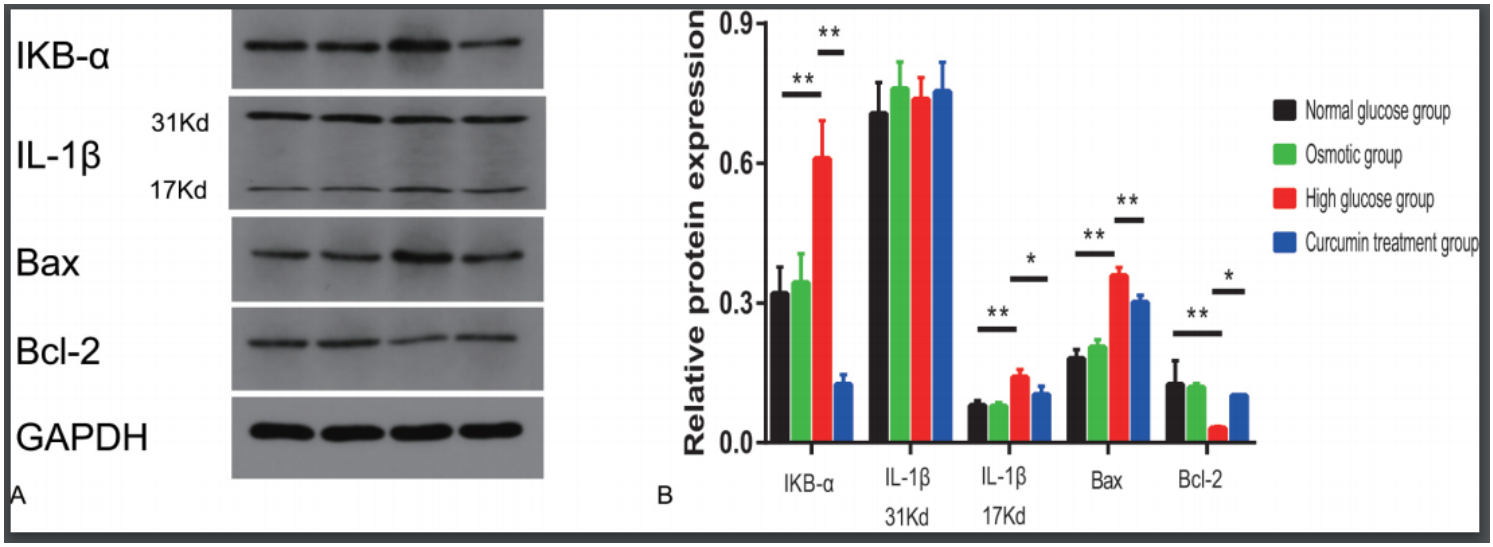

Figure 6

Comparison of IKb-α、IL-β、Bax and Bcl-2 proteins expression in RRVECs in each group. *P<0.05 **P<0.01 A. Electropherogram of IKb-α、 IL-β、Bax and Bcl-2 protein expressions; (B) Histogram of IKb-α、IL-β、Bax and Bcl-2 protein expressions